ELSEVIER

Journal of Alloys and Compounds 408–412 (2006) 307–312

Journal of ALLOYS AND COMPOUNDS

www.elsevier.com/locate/jallcom

Large magnetocaloric effects and thermal transport properties of $La(FeSi)_{13}$ and their hydrides

K. Fukamichi *, A. Fujita, S. Fujieda

Department of Materials Science, Graduate School of Engineering, Tohoku University, Aoba-yama 02, Sendai 980-8579, Japan

Available online 20 July 2005

Abstract

$La(Fe_xSi_{1-x})_{13}$ exhibit an itinerant-electron metamagnetic (IEM) transition at relatively low applied magnetic fields just above the Curie temperature T_C. Large magnetocaloric effects (MCEs) in terms of the isothermal temperature change ΔS_m and the adiabatic temperature change ΔT_{ad} are followed by the IEM transition. The MCEs increase, while T_C decreases with increasing Fe concentration. Therefore, T_C of these compounds should be controlled up to room temperature from the viewpoint of practical applications. The working temperature as magnetic refrigerants is extended from about 185 to 330 K by adjusting hydrogen concentration. After hydrogen absorption, the MCEs as well as the thermal conductivity of $La(Fe_xSi_{1-x})_{13}$ and their hydrides exhibit excellent characteristics in the temperature range mentioned above. Consequently, the present compounds are one of the promising candidates for magnetic refrigerants working in a wide temperature range covering room temperature.

Keywords: Itinerant-electron metamagnetic (IEM); Magnetocaloric effects (MCEs); Room temperature

1. Introduction

Recently, magnetic materials including rare-earth elements and compounds have attracted much attention in development of room temperature magnetic refrigerants having large magnetocaloric effects (MCEs) such as the large isothermal entropy change and the adiabatic temperature change [1]. For example, Gd was adopted for a room temperature magnetic refrigerant in demonstration [2,3]. High-efficiency magnetic refrigerations will achieve abolition of environmental hazardous Freon-based gases and also facilitation of the energy-saving in cooling technologies. For these purposes, materials with the magnetic field induced first-order transition are advantageous in utilization of the latent heat of the transition. Among magnetic rare-earth-based compounds, $Gd_5Ge_2Si_2$ is one of recent candidates, because of its large MCEs due to the magnetic phase transition induced by the first-order crystallographic structural transformation around room temperature [4].

It should be also mentioned that many compounds consisted of rare-earth and 3d transition metals have been reported to exhibit various magnetic phase transition related to the itinerant character of 3d electrons [5]. Recently, it has been demonstrated that $La(Fe_xSi_{1-x})_{13}$ in the concentration range $0.86 \leq x \leq 0.90$ show the thermal-induced first-order magnetic phase transition from the ferromagnetic (F) to the paramagnetic (P) phase at the Curie temperature T_C around 200 K. The magnetic field induced first-order transition from the P to the F phase also occurs just above T_C in relatively low magnetic fields, which is known as the itinerant-electron metamagnetic (IEM) transition [6–9]. It has been also confirmed that the large MCEs are followed by the IEM transition [10–13]. Therefore, the increase of T_C up to room temperature makes the present compounds applicable to the magnetic refrigerants showing the large MCEs in relatively low magnetic fields at wide temperature ranges covering room temperature. It has been reported that T_C is increased by hydrogen absorption in $La(Fe_xSi_{1-x})_{13}$ up to room temperature with keeping the IEM transition [14–16].

In the present paper, the influence of hydrogen absorption on T_C and the MCEs of $La(Fe_xSi_{1-x})_{13}$ and their hydrides

* Corresponding author.
E-mail address: fukamich@tagen.tohoku.ac.jp (K. Fukamichi).

0925-8388/$ – see front matter © 2005 Elsevier B.V. All rights reserved.
doi:10.1016/j.jallcom.2005.04.022

are evaluated. Furthermore, the thermal transport property is discussed from the viewpoint of practical applications.

2. Experiments

$La(Fe_xSi_{1-x})_{13}$ were prepared by arc-melting in an argon gas atmosphere. To homogenize the specimens, the heat treatment was carried out in a vacuum quartz tube at 1323 K for 10 days. The hydrogen absorption was made out by annealing in a hydrogen atmosphere by using a closed chamber. The magnetization was measured with a superconducting quantum interference device (SQUID) magnetometer. For direct measurements of adiabatic temperature change, the specimens were put into a thermal insulation holder made of a quartz and moved quickly between the inside and the outside of a superconducting solenoid. The temperature of the specimen was measured with a resistance thermometer having four manganin terminals with low thermal conductivity. Thermal conductivity measurements were carried out by a pulse method.

3. Results and discussion

Fig. 1 shows thermomagnetization curves in 0.3 T for $La(Fe_{0.88}Si_{0.12})_{13}$ measured during the 1st, 2nd and 10th temperature cycles between 192 and 200 K. The annealed specimen was cooling down from room temperature to 185 K before the first cycle. A steep change in magnetization M appears around 195.5 and 194.5 K in the heating and cooling processes, respectively, of the first cycle. Therefore, the hysteresis width of the thermal-induced first-order transition between the ferromagnetic and the paramagnetic states is within 1 K at 0.3 T. As seen in Fig. 1, no shifts of the F–P and P–F transition temperature are caused by the thermal cycles. For application as magnetic refrigerants, it is desired that the first-order transition should be

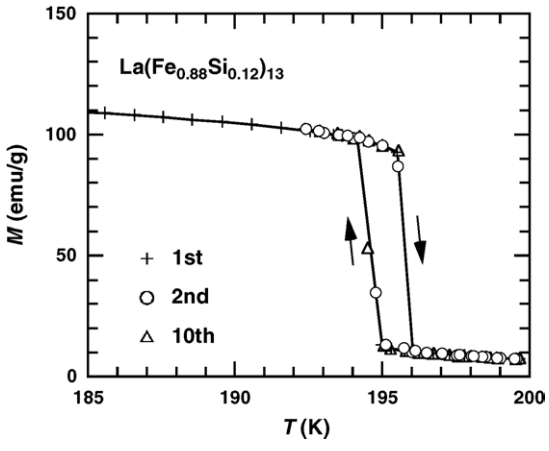

Fig. 1. Thermomagnetization curves of $La(Fe_{0.88}Si_{0.12})_{13}$ measured during the 1st, 2nd and 10th temperature cycles between 192 and 200 K.

stable against cycle running of refrigerators. It has been found that $Fe_{49}Rh_{51}$ exhibits large magnetocaloric effects, namely the isothermal entropy change $\Delta S_m = -12$ J/kg K and $\Delta T_{ad} = 8$ K in magnetic field change ΔB of 0–2 T, due to the first-order antiferromagnetic–ferromagnetic transition accompanied by the lattice distortion around room temperature [17,18]. However, large MCEs in $Fe_{49}Rh_{51}$ are drastically reduced by the irreversible transition after thermal cycles [18]. In $Gd_5Ge_2Si_2$, another candidate for magnetic refrigerants, the gradual shift of the transition temperature by thermal cycles has been observed because of the martensitic-like structural transformation coming up with the magnetic phase transition, although large MCEs are conserved in the thermally cycled specimens [19]. On the other hand, according to temperature and magnetic field scan measurements of X-ray diffraction [9,20], no crystalline structural transformation is induced by the thermal induced and the IEM transitions in $La(Fe_{0.88}Si_{0.12})_{13}$, though the isotropic volume magnetostriction larger than 1% is caused by the IEM transition [7–9,20]. Therefore, the transition stability against thermal cycle is much excellent, compared to the materials having the structural transformation transition mentioned above.

According to the Maxwell relation, the isothermal entropy change is related with the thermal variation of magnetization as

$$\Delta S_m = \int_0^{H_{max}} \mu_0 \left(\frac{\partial M}{\partial T}\right) dH \quad (1)$$

with $B = \mu_0 H$, where μ_0, B and H are permeability, magnetic flux density and magnetic field, respectively. The magnetization around the Curie temperature T_C exhibits a steep change due to the first-order phase transition as shown in Fig. 1. Furthermore, the temperature dependence of the critical field of the IEM transition gives a monotonic increase [12], therefore, the F state exists up to higher temperature ranges by applying magnetic fields and a large $\partial M/\partial T$ due to the thermal-induced transition is obtained at higher temperatures with increasing the strength of applied magnetic fields. Accordingly, a large ΔS_m is expected in temperature ranges above T_C. By applying Eq. (1) to the isothermal magnetization data, the temperature dependence of ΔS_m is evaluated. The hysteresis is also observed in the isothermal magnetization curves due to the IEM transition. By regarding M as a function of T and B, the thermal variations of ΔS_m in the magnetic field change from 0 to 2 T ($\Delta B = 2$ T) and from 2 to 0 T ($\Delta B = -2$ T) are obtained for $La(Fe_xSi_{1-x})_{13}$ ($x = 0.88$ and 0.90) as given in Fig. 2. As expected from Eq. (1) and the data displayed in Fig. 1, a steep increase of ΔS_m appears in negative and positive directions with respect to $\Delta B = 2$ and -2 T around $T_C = 195$ K for $x = 0.88$, bringing about a maximum value of $|\Delta S_m| = 20$ J/(kg K). The $|\Delta S_m|$–T curve for $x = 0.88$ shows a slight decrease between 195 and 203 K, then the value is remarkably reduced to almost zero above 204 K. In the $La(Fe_xSi_{1-x})_{13}$ compounds, T_C decreases with increasing Fe concentration [9]. For $x = 0.90$, the value of T_C is 183K, accordingly, a large $|\Delta S_m|$

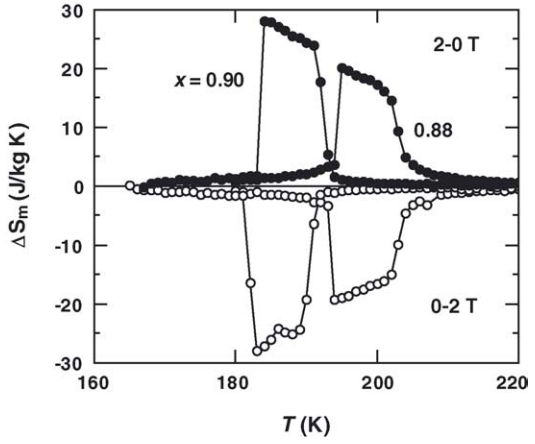

Fig. 2. Temperature dependence of the isothermal entropy change ΔS_m for $La(Fe_xSi_{1-x})_{13}$ ($x = 0.88$ and 0.90) in the magnetic field change from 0 to 2 T and from 2 to 0 T.

is observed in lower temperature range, compared to that for $x = 0.88$. That is, the magnitude of $|\Delta S_m| = 28$ J/(kg K) for $x = 0.90$ is about 1.4 times larger than that for $x = 0.88$. For both the compounds with $x = 0.88$ and 0.90, the steep change of $|\Delta S_m|$ in $\Delta B = 2$ T appears at lower temperatures than that in $\Delta B = -2$ T. The difference in the temperature range for large ΔS_m with respect to sign of ΔB is 1–2 K. Such hysteresis width is smaller than the adiabatic temperature change (see Fig. 3(a and b)). It should be stressed that the maximum value of ΔS_m for the present compounds with

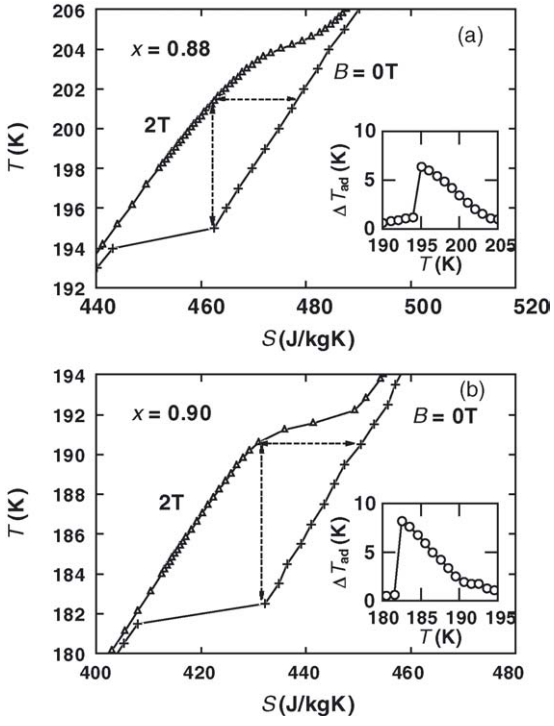

Fig. 3. Temperature vs. entropy curves in magnetic fields of 0 and 2 T for: (a) $x = 0.88$ and (b) $x = 0.90$. The insets in (a and b) show temperature dependence of the adiabatic temperature change ΔT_{ad} for $x = 0.88$ and 0.90, respectively.

$\Delta B = 2$ T is comparable or superior to the values in other candidates such as $Gd_5Ge_2Si_2$ with $\Delta S_m = -28$ J/(kg K) [21] and $MnFeAs_{0.5}P_{0.5}$ with $\Delta S_m = -16$ J/(kg K) [22].

For high-efficiency cooling cycles, not only a large ΔS_m but also a large adiabatic temperature change ΔT_{ad} is necessary. The relation between ΔT_{ad} and ΔS_m is expressed as

$$\Delta T_{ad} = -\int_0^B \frac{T}{C_B}\frac{\partial S}{\partial B}\,dB \approx -\frac{T}{C_B}\Delta S_m \quad (2)$$

where C_B is the total specific heat under magnetic field [1]. Therefore, ΔT_{ad} is proportional to ΔS_m, but the magnitude of ΔT_{ad} is not defined until C_B is determined. The value of ΔT_{ad} is also evaluated from the simpler following relation [1]:

$$\Delta T_{ad} = [T(S)_B - T(S)_0]_S \quad (3)$$

where $T(S)$ is the temperature as a function of entropy S. Therefore, ΔT_{ad} is evaluated from heat capacity data under magnetic field. Shown in Fig. 3(a and b) are the T–S curves in $B = 0$ and 2 T for $x = 0.88$ and 0.90, respectively. The vertical arrows indicate the magnitude of ΔT_{ad} at T_C. The T–S curve for $x = 0.88$ in the P state in 0 T shows a similar variation to that for $x = 0.90$. Therefore, a wider area is enclosed by the T–S curves due to larger ΔS_m for $x = 0.90$ compared to those for $x = 0.88$, as indicated by the horizontal arrows. The temperature dependence of ΔT_{ad} obtained from Eq. (3) for $x = 0.88$ and 0.90 is displayed in the inset of Fig. 3(a and b), respectively. For $x = 0.88$, the maximum value of ΔT_{ad} of about 6.5 K is observed at T_C and ΔT_{ad} gradually decreases with increasing temperature because the T–S curve in 2 T approaches to that in 0 T. On the other hand, the maximum value of $\Delta T_{ad} = 8.1$ K is observed for $x = 0.90$. The decreasing rate of ΔT_{ad} above T_C for $x = 0.90$ is slightly larger than that for $x = 0.88$, because value of $T_C|_{B=2\,T}$ is close to the sum of $T_C|_{B=0\,T} + \Delta T_{ad}$ for $x = 0.90$ as shown in Fig. 3(b).

Based on the Brayton cycle, the active magnetic regenerator (AMR) type refrigerator has recently been proposed as a most practical refrigeration scheme [1,3]. In the AMR refrigerator, magnetic materials with different working temperature range can be combined to expand the whole working temperature range of refrigerator [1]. Therefore, by controlling T_C of the $La(Fe_xSi_{1-x})_{13}$ compounds up to room temperature with keeping the IEM transition, the present compound system can be used as magnetic refrigerants in the range from 180 K to room temperature. According to our recent researches, the magnetovolume effects in the present compounds are very large [7–9,23,24]. For instance, the volume in the F state is larger than that in the P state due to the spontaneous volume magnetostriction [8,9]. Furthermore, T_C of the $La(Fe_xSi_{1-x})_{13}$ compounds is sensitive to external hydrostatic pressure [9,24] because the magnetic properties of the present compounds are dominated by characteristics of Fe 3d electron band structures [23]. Therefore, the increase of T_C is connected with the lattice constant with keeping the characteristic band structure. It has

been known that hydrogen is easily absorbed in rare-earth 3d transition metal-based compounds and hydrogen atoms in the interstitial positions expand the lattice parameter. In fact, $La(Fe_{0.88}Si_{0.12})_{13}H_y$ have been readily prepared by annealing in hydrogen atmosphere [12–16].

From the magnetization measurements, T_C exhibits a linear increase with the hydrogen concentration y. At the present stage, the highest value of T_C is found to be about 330 K in $La(Fe_{0.88}Si_{0.12})_{13}H_{1.6}$. After hydrogen absorption, the transition at T_C is still the first-order and the IEM transition occurs above T_C. Therefore, hydrogenated $La(Fe_{0.88}Si_{0.12})_{13}H_y$ are also expected to exhibit large MCEs. Practically, magnetic refrigerants are desired to have not only a large ΔS_m but also a large refrigerant capacity q defined by

$$q = \int_{T_1}^{T_2} \Delta S_m \, dT \tag{4}$$

where q is a measure of how much heat can be transferred between thermal baths at T_1 and T_2 in one ideal refrigeration cycle [25]. Fig. 4 displays the variation of ΔS_m and q plotted against T_C for various hydrogen concentration y for $La(Fe_{0.88}Si_{0.12})_{13}H_y$. For comparison, the data for $La(Fe_{0.90}Si_{0.10})_{13}H_y$ ($y = 0.0$ and 1.0) are also plotted. It is noteworthy that ΔS_m in $\Delta B = 2$ T is unchanged after T_C is elevated by hydrogen absorption. As seen from Eq. (1), ΔS_m is significantly influenced by change in M at T_C. The value of T_C at the first-order transition is determined by equality of the Gibbs energy in the F and P states, therefore, increase of T_C does not necessarily mean the increase of the magnetic moment in the F state. It has been reported that hydrogen absorption in the present compounds results in not only increase of T_C but also increase of spin-wave dispersion coefficient [26]. In other words, the thermal demagnetization becomes smaller in the $La(Fe_xSi_{1-x})_{13}H_y$ having higher T_C with increasing y. As a result, the magnetization in the F state at T_C is almost the same even though the F state persists up to higher temperatures, resulting in unchanged value of ΔS_m.

When one of the magnetic refrigerants is embedded in a refrigerator, T_1 and T_2 in Eq. (4) are regarded as the temperatures of the hot and cold sinks, respectively [25]. On the other hand, in the refrigerator with plural magnetic refrigerants, the heat transfer by magnetic refrigerants with lower working range is cascaded to other refrigerants with higher working range, resulting in the extension of whole working temperature ranges [1]. Therefore, to evaluate the value of q in the $La(Fe_xSi_{1-x})_{13}H_y$ compounds with a certain hydrogen concentration, T_C is regarded as T_1, and furthermore, the temperature span T_2–T_1 is settled to be the same magnitude of ΔT_{ad} in $\Delta B = 2$ T. Because of the large ΔS_m as well as a plateau-like behavior of ΔS_m–T curve above T_C for the $La(Fe_{0.88}Si_{0.12})_{13}H_y$ compounds, the refrigerant capacity q reaches to about −130 J/kg, which is almost the same in magnitude with data calculated from ΔS_m in the literates for $Gd_5Ge_2Si_2$ [21] and $MnFeAs_{0.5}P_{0.5}$ [22]. Furthermore, the value of q is enhanced as well as ΔS_m with increasing Fe concentration as seen from the data for $La(Fe_{0.90}Si_{0.10})_{13}H_y$ in Fig. 5. Such steady value of q against increase of T_C is favorable for construction of the cascade system by combining the $La(Fe_xSi_{1-x})_{13}H_y$ compounds with different y, bringing about extension of the working temperature range.

The value of ΔT_{ad} and the thermally normalized value $\Delta T_{ad}/T$ are plotted against T_C in $\Delta B = 2$ T for the $La(Fe_{0.88}Si_{0.12})_{13}H_y$ ($y = 0.0$, 0.5, 1.0 and 1.5) compounds in Fig. 5. For comparison, the data for $La(Fe_{0.90}Si_{0.10})_{13}H_y$ ($y = 0.0$ and 1.0) are also shown in the same figure. The value of ΔT_{ad} is located around 6.5 K after controlling T_C in a temperature range between 195 and 320 K for the $La(Fe_{0.88}Si_{0.12})_{13}H_y$ compounds. As seen from Fig. 3(a and b), the phonon contribution is less sensitive to the Fe concentration than that of ΔS_m. Similar situation appears after hydrogen absorption, resulting in a larger value of ΔT_{ad} for $La(Fe_{0.90}Si_{0.10})_{13}H_y$ than that for the $La(Fe_{0.88}Si_{0.12})_{13}H_y$ compounds in whole temperature range. From the relation between ΔT_{ad} and ΔS_m derived from Eq. (2), $\Delta T_{ad}/T$ is given by the following expression including the total specific heat

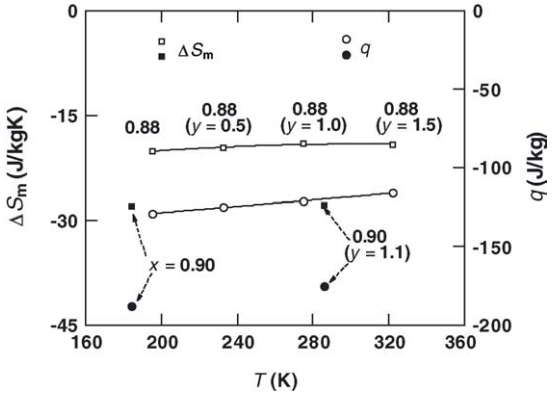

Fig. 4. The isothermal entropy change ΔS_m and the refrigerant capacity q in $\Delta B = 2$ T plotted against T_C for various hydrogen concentration y in $La(Fe_{0.88}Si_{0.12})_{13}H_y$. The data of $La(Fe_{0.90}Si_{0.10})_{13}H_y$ ($y = 0.0$ and 1.0) are also shown, for comparison.

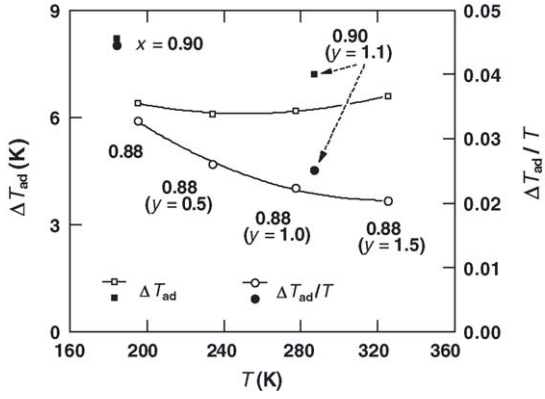

Fig. 5. The adiabatic temperature change ΔT_{ad} and the thermally normalized value $\Delta T_{ad}/T$ plotted against T_C in $\Delta B = 2$ T for $La(Fe_{0.88}Si_{0.12})_{13}H_y$ ($y = 0.0$, 0.5, 1.0 and 1.5) compounds. The data of $La(Fe_{0.90}Si_{0.10})_{13}H_y$ ($y = 0.0$ and 1.0) are also shown, for comparison.

C_B in the magnetic fields.

$$\frac{\Delta T_{ad}}{T} = -\frac{\Delta S_m}{C_B} \quad (5)$$

The value of C_B becomes large around room temperature due to the phonon contribution of the lattice part, which is not controlled by magnetic field. Accordingly, the heat change due to ΔS_m is reduced by the thermal load of the lattice part and $\Delta S_m/C_B$ represents the ratio between the cooling power and the lattice thermal load at a certain temperature [1]. Although a slight decrease of $\Delta T_{ad}/T$ is observed with increasing T_C in both $La(Fe_{0.88}Si_{0.12})_{13}H_y$ and $La(Fe_{0.90}Si_{0.10})_{13}H_y$, $\Delta T_{ad}/T$ around room temperature still keeps its value of about 0.02–0.03, large enough to expect high efficiency in an AMR refrigerator [1].

The heat transfer in the magnetic refrigerator is a dynamic process, therefore, the local thermodynamic equilibrium state is scarcely maintained [27]. In adiabatic processes for the second-order phase transition, the thermodynamic change is achieved in the time scale of spin-lattice relaxation rate. Therefore, the adiabatic temperature change is achieved even in the dynamic process of the refrigerators. On the other hand, the first-order phase transition proceeds with going over the energy barrier between the F and P states, resulting in the nucleation and growth phenomena. The time scale of adiabatic process related to the nucleation and growth is unknown in a priori, consequently the direct measurement of adiabatic temperature change is necessary by taking time scale into account. The directly observed adiabatic temperature change ΔT_{ad}^{d} is brought within 1.5 s after producing the magnetic field change, therefore, it is revealed that the adiabatic process in the present compound is achieved smoothly. It has been reported that the temperature dependence of ΔT_{ad}^{d} is similar to that of the value of ΔT_{ad} estimated from the specific heat measurement except for a slightly smaller maximum value due to the incomplete thermal isolation in the present experiment. However, taking non-equilibrium condition in the actual refrigerator into account, the maximum value of ΔT_{ad}^{d} of 5.9 K in $\Delta B = 2$ T is expected to be large enough for practical applications.

In real actions of AMR refrigerators, thermodynamic irreversible processes take place and an additional entropy is generated within one refrigeration cycle [1]. The additional entropy is generated by mainly three terms, i.e., the dissipation of flow energy of heat transfer fluid, the axial heat conduction along the regenerator through the AMR bed retaining magnetic refrigerants between hot and cold sinks, and the finite heat transfer between fluid and the magnetic refrigerants [1]. The entropy generations due to the former two terms are reduced by keeping enough porosity in the bed, and by lowering the effective heat capacity of fluid than that of the bed. To reduce the third-term, the thermal conductivity of the magnetic refrigerants should be larger compared to heat flow of fluid. Therefore, it is necessary to measure the thermal conductivity κ of the magnetic refrigerants to construct the high-efficiency refrigerators. As shown in Fig. 6, κ around

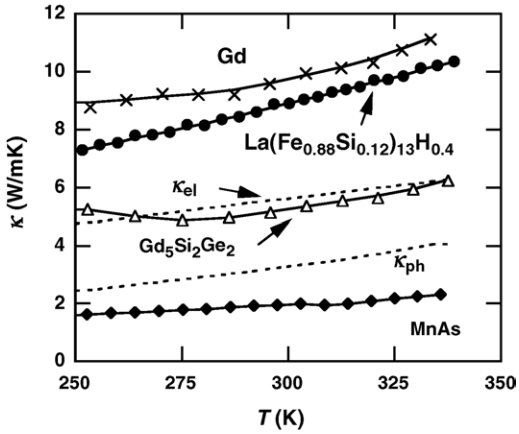

Fig. 6. Temperature dependence of thermal conductivity κ for $La(Fe_{0.88}Si_{0.12})_{13}H_{0.4}$, together with the calculated values of the electronic (κ_{el}) and phonon (κ_{ph}) contributions given by the dotted lines. The values of κ for $Gd_5Ge_2Si_2$ and MnAs are also plotted, for comparison.

room temperature for the $La(Fe_{0.88}Si_{0.12})_{13}H_{0.4}$ is almost the same in magnitude with that of Gd metal, whereas the values of κ for other candidates such as $Gd_5Ge_2Si_2$ [28] and MnAs [28] are much smaller in this temperature range. The total value of κ is expressed as the sum of the electronic part κ_{el} and the phonon part κ_{ph}. Furthermore, the electronic part κ_{el} is related to the electrical resistivity ρ as given by the following Wiedeman–Franz law:

$$\kappa_{el} = \frac{LT}{\rho} \quad (6)$$

where L is the constant value of 2.45×10^{-8} W Ω/K^2. From the ρ–T data, κ_{el} for the present compound is calculated to be about 60% of the total value of κ around room temperature. The thermal variations of κ_{el} and κ_{ph} calculated for $La(Fe_{0.88}Si_{0.12})_{13}$ are also displayed in Fig. 6. The total values of κ of $Gd_5Ge_2Si_2$ and MnAs are, respectively, almost the same as κ_{el} and smaller than κ_{ph} of $La(Fe_{0.88}Si_{0.12})_{13}$. For both $Gd_5Ge_2Si_2$ and MnAs, the Debye temperature θ_D lies about 220–250 K [29,30], while θ_D is about 350 K for $La(Fe_{0.88}Si_{0.12})_{13}$, therefore, thermal decay of κ_{ph} due to the Umklapp phonon scattering is relatively smaller in $La(Fe_{0.88}Si_{0.12})_{13}$. Furthermore, covalent or ionic characters of atoms in $Gd_5Ge_2Si_2$ and MnAs would reduce the electronic contribution to thermal conductivity. In consequence, the thermal conductivity of the present compound is better for reduction of entropy generated by finite heat transfer between the magnetic refrigerant and the heat exchange fluid.

Finally, it should be emphasized that the elements of the present compounds are very cheap economically and also completely harmless for human life.

4. Conclusion

The magnetic properties and magnetocaloric effects, together with thermal conductivity have been investigated for

$La(Fe_xSi_{1-x})_{13}$ itinerant-electron metamagnetic (IEM) compounds and their hydrides. The Curie temperature T_C for the first-order transition from the ferromagnetic (F) to the paramagnetic (P) states of $La(Fe_{0.88}Si_{0.12})_{13}$ is scarcely influenced by thermal cycles, T_C is increased from 195 K for $y = 0$ to 330 K for $y = 1.6$. After controlling T_C by hydrogen absorption, the IEM transition is confirmed to be preserved, resulting in large magnetocaloric effects (MCEs) as well as the refrigerant capacity even in the relatively low magnetic field of 2 T at a range of temperature 180–330 K. From the direct measurements, a large value of adiabatic temperature change is confirmed to be obtainable in practical non-equilibrium cooling processes. In addition, the thermal conductivity of $La(Fe_xSi_{1-x})_{13}H_y$ is better than that of other candidates. Consequently, the $La(Fe_xSi_{1-x})_{13}H_y$ are one of the most practical candidates for magnetic refrigerants working in a wide temperature range.

References

[1] A.M. Tishin, Y.I. Spichkin, The Magnetocaloric Effect and its Applications, Series in Condensed Matter Physics, IOP, London, 2003.
[2] G.V. Brown, J. Appl. Phys. 47 (1976) 3673.
[3] C. Zimm, A. Jastrab, A. Sternberg, V.K. Pecharsky, K.A. Gschneidner Jr., M. Osborne, I. Anderson, Adv. Cryog. Eng. 43 (1998) 1759.
[4] V.K. Pecharsky, K.A. Gschneidner Jr., Phys. Rev. Lett. 78 (1997) 4494.
[5] H.R. Kirchmayr, C.A. Poldy, in: K.A. Gschneidner Jr., L. Eyring (Eds.), Handbook on the Physics and Chemistry of Rare Earths, vol. 2, North-Holland, Amsterdam, 1979, p. 55 (Chapter 14).
[6] A. Fujita, Y. Akamatsu, K. Fukamichi, J. Appl. Phys. 85 (1999) 4756.
[7] K. Fukamichi, A. Fujita, J. Mater. Sci. Technol. 16 (2000) 167.
[8] A. Fujita, K. Fukamichi, IEEE Trans. Magn. 35 (1999) 3796.
[9] A. Fujita, S. Fujieda, K. Fukamichi, H. Mitamura, T. Goto, Phys. Rev. B 65 (2002) 014410.
[10] S. Fujieda, A. Fujita, K. Fukamichi, Y. Yamazaki, Y. Iijima, Appl. Phys. Lett. 81 (2002) 1276.
[11] A. Fujita, S. Fujieda, K. Fukamichi, Y. Yamazaki, Y. Iijima, Mater. Trans. 43 (2002) 1202.
[12] A. Fujita, S. Fujieda, Y. Hasegawa, K. Fukamichi, Phys. Rev. B 67 (2003) 104416.
[13] S. Fujieda, A. Fujita, K. Fukamichi, Sci. Technol. Adv. Mater. 4 (2003) 339.
[14] A. Fujita, S. Fujieda, K. Fukamichi, Y. Yamazaki, Y. Iijima, Trans. Mater. Res. Soc. Jpn. 26 (2001) 219.
[15] S. Fujieda, A. Fujita, K. Fukamichi, Appl. Phys. Lett. 79 (2001) 653.
[16] K. Fukamichi, A. Fujita, S. Fujieda, in: D. Chandra, R.G. Bautista, L. Schlapbach (Eds.), Advanced Materials for Energy Conversion II, The Minerals, Metals and Materials Society, USA, 2004, p. 265.
[17] S.A. Nikitin, G. Myalikgulyev, A.M. Tishin, M.P. Annaorazov, K.A. Asatryan, A.L. Tyurin, Phys. Lett. A 148 (1990) 363.
[18] M.P. Annaorazov, S.A. Nikitin, A.L. Tyurin, K.A. Asatryan, A.K. Dovletov, J. Appl. Phys. 79 (1996) 1689.
[19] E.M. Levin, A.O. Pecharsky, V.K. Pecharsky, K.A. Gschneidner Jr., Phys. Rev. B 63 (2001) 064426.
[20] A. Fujita, K. Fukamichi, K. Koyama, K. Watanabe, J. Appl. Phys. 95 (2004) 6687.
[21] A.O. Pecharsky, K.A. Gschneidner Jr., V.K. Pecharsky, J. Appl. Phys. 93 (2003) 4722.
[22] O. Tegus, E. Brück, L. Zhang, W. Dagula, K.H.J. Buschow, F.R. de Boer, Physica B 319 (2002) 174.
[23] A. Fujita, K. Fukamichi, J.-T. Wang, Y. Kawazoe, Phys. Rev. B 68 (2003) 104431.
[24] A. Fujita, K. Fukamichi, M. Yamada, T. Goto, J. Appl. Phys. 93 (2003) 7263.
[25] V.K. Pecharsky, K.A. Gschneidner Jr., J. Appl. Phys. 90 (2001) 4614.
[26] A. Fujita, S. Fujieda, K. Fukamichi, J. Alloy Compd., in press.
[27] J.A. Barclay, J. Alloy Compd. 207–208 (1994) 355.
[28] S. Fujieda, Y. Hasegawa, A. Fujita, K. Fukamichi, J. Appl. Phys. 95 (2004) 2429.
[29] U.V. Serdyuk, R.P. Krentsis, P.V. Geld, J. Less-Common Metals 111 (1985) 347.
[30] F. Grønvold, S. Snildal, E. Westrum, Acta Chem. Scand. 24 (1970) 285.